

Voltage Control in Distribution System Considering The Impact of PV Generation Using MPPT Controller on Tap Changers and Autonomous Regulators

^[1] R.Madhan Mohan ^[2] P.Bhaskara Prasad ^[3] O.Lakshmi Narasimha Kesavulu
^{[1][2]} Assistant Professor, ^[3] PG Student,
^{[1][2][3]} Dept of EEE, Annamacharya Institute Of Technology & Sciences, Rajampet, AP, India.

Abstract: — The renewable policies in various countries are driving significant growth of grid connected renewable generation sources such as Solar Photovoltaic (PV), wind, biomass, Fuel Cell (FC), or micro turbines. Among all the proportion of photovoltaic (PV) generation into existing power system generation mix has significantly increased in recent times. Most of the PV plants are getting connected to low/medium voltage distribution level as distributed generation (DG). The uptake of an intermittent power from the PVs is challenging the power system operation and control. The network voltage control is one of the major challenges during the operation of the distribution connected PVs. The active power injection from a PV plant causes variable voltage rise. This forces the existing voltage control devices such as on-load tap-changer (OLTC) and voltage regulator (VR) to operate continuously. The consequence is the reduction of the operating life of the voltage control mechanism. Also, the conventional non coordinated reactive power control results in the operation of the VR at its control limit (VR runaway condition). But the existing methods are does not consider detailed impact of DG such as PV on autonomous local control setting of voltage regulator. This paper proposes a new technique for voltage regulation of a radial medium (MV) distribution system in presence of distribution generation (DG) units. The proposed technique consists of the coordinated actions of on-load tap changer (OLTC) of transformer and reactive power coordination in the distribution network by the impact of PV generation. Simulation results reveal that the proposed control method is capable of maintaining the system voltage within the permitted range.

Index Terms— Distribution networks, photovoltaics (PV), reactivepower optimization, voltage control.

I. INTRODUCTION

Solar photovoltaic distributed generation (PV-DG) systems are one of the fastest-growing types of renewable energy sources being integrated worldwide onto distribution systems. The cumulative global capacity of PV generation is expected to grow up to 200GWp by the year 2017. The cumulative global installed capacity is approximately 137GW, till the end of 2013. PV plants are integrated both at the transmission level and the distribution level from the power system integration point of view. Most of the PV plants are getting connected to low/medium voltage distribution level as distributed generation (DG). However, PV-DG impacts on distribution systems can

be either steady-state or dynamic in nature, and they include:

- ◆ Changes in feeder voltage profiles, including voltage rise and unbalance.
- ◆ Changes in feeder loading, including potential equipment and component overload.
- ◆ Frequent operation of voltage-control and regulation devices, such as load tap changers (LTCs), line voltage regulators (VRs), and capacitor banks
- ◆ Reactive-power flow fluctuations due to operation of switched capacitor banks
- ◆ Overvoltage issues can allow the DGs to absorb reactive power
- ◆ Power quality, PV-DG intermittency may lead to voltage fluctuation issues.

**International Journal of Engineering Research in Electrical and Electronic
Engineering (IJEREEE)
Vol 3, Issue 3, March 2017**

The severity of these impacts varies with the penetration level, the location of the PV-DG, and the electrical characteristics of the distribution systems. For instance, a high PV-DG penetration level could cause a feeder to become an active circuit and inject power back to the transmission system. This high penetration condition may affect voltage profiles, over current protection, and capacitor-bank operation. Such a situation may occur on feeders selected for integrating multiple utility-scale PV-DG plants. Because both PV-DG output and feeder load vary throughout the day, it is necessary to investigate impacts for different degrees of penetration of PV-DG and also to assess the effects under various conditions of feeder loading. The injection of PV generator active power impacts the operation of OLTCs and VRs. Present day voltage control practices do not consider detailed impacts of PVs on these voltage control mechanisms. This paper presents the detailed analysis of the impact PV on OLTCs and VRs and reactive power coordination. Various voltage regulation strategies to tackle the possible adverse impact of PVs are also developed.

II. SYSTEM MODELING

The capacity of a PV plant determines the voltage level at which it should be integrated. The PV generation is getting integrated mostly at the low voltage and the medium voltage distribution level. The grid integration standards are evolving in various countries in order to achieve a seamless integration. The PV plants need to comply with the various technical requirements prescribed in a grid integration standard. The set of technical requirements depend upon the voltage level at which the PV plant is getting integrated. The power system operators in different countries have developed the country specific guidelines in the integration standards. The operation of a PV generation at an unity power factor means no contribution from a PV inverter towards the reactive power or the voltage support functionality. The network operators are increasingly demanding a contribution from PV generators towards steady state voltage control functionality. The voltage support functionality by PV plant can be offered by an active power curtailment and a reactive power support. The contribution of a reactive power at the highest active power capacity of a PV plant necessitates an interface inverter overrating. This is indicated in terms of a PV generation capacity curve in Fig.1. The grid codes usually recommend a power factor range as shown in the capacity curve at which PV

plant should be able to operate even at its maximum active power capacity. This determines an apparent power rating of a PV inverter must be able to operate at 0.95 lead/lag power factor(Pf).

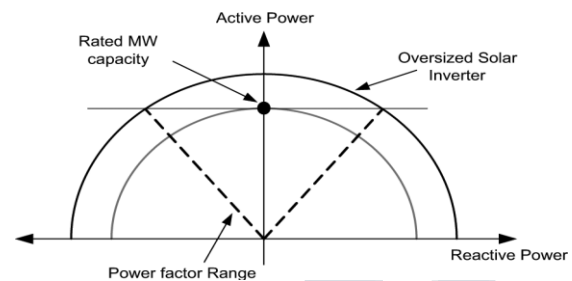


Fig. 1. Solar generation capacity curve.

A typical topology of a grid integrated PV and a control structure of its power inverter is shown in Fig.2. The topology comprises three main subsystems: a PV panel, a grid interface power converter and a converter control system. A PV panel converts solar energy into dc electrical energy. The dc electrical energy generated from a PV panel is injected into a power system at the nominal grid voltage and the nominal grid frequency by utilizing a power electronic converter. The control structure of a power converter ensures an efficient operation and also incorporates the grid support features.

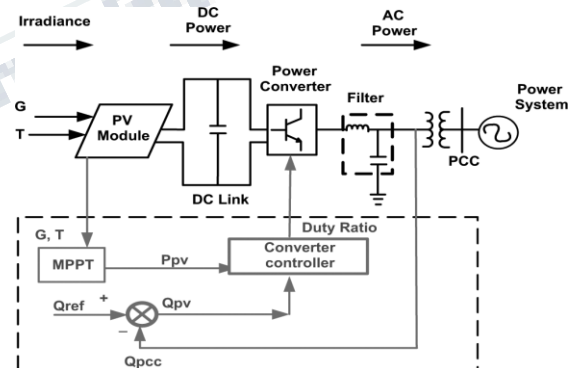


Fig. 2. Generic grid-integrated PV topology.

Fig.3. is a simple equivalent circuit of a radial feeder. The feeder has a connected load and a PV generator. The active/reactive power consumption by a load and the active power injection by a PV both will cause a voltage drop on a feeder. This voltage drop can be mathematically derived as follows. In Fig.3. V1 is a constant substation voltage. The vector diagram of the operation of feeder is shown in Fig.4.

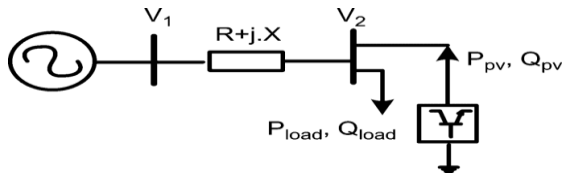


Fig. 3. PCC voltage control by PV plant.

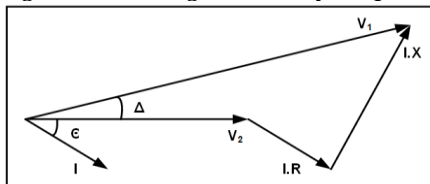


Fig.4. Vector diagram of radial feeder

The On-load tap changer (OLTC) is primarily responsible for feeder voltage control. OLTCs are typically installed in the substation from where a feeder emanates. The typical voltage control mechanism in an OLTC is represented in Fig.5. An operator will specify the particular voltage set point to control the voltage of a regulated bus. The turns ratio of a transformer can be adjusted in steps from the transformer windings. The OLTC controls the voltage of the regulated bus within the defined dead band settings. The regulated bus voltage is compared with user defined set point by the comparator. The tap is not varied if the measured voltage is within the dead band. The taps are moved after an operator defined time delay if the measured voltage is outside the dead band.

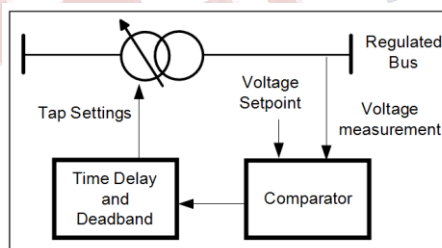


Fig.5. OLTC Voltage Control mechanism.

A VR is typically an autotransformer with $\pm 10\%$ voltage regulation capability. The VR maintains the load terminal voltage at the set value by adjusting the tap position as the load current varies. The deadband and the delay time concept is similar to the OLTC. The typical VR schematic diagram is shown in Fig.6.

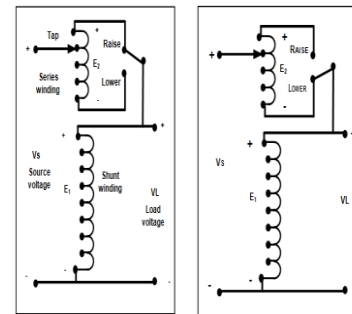


Fig.6. Voltage regulator.

A typical MV radial distribution feeder under consideration here. This feeder has PV along with its reactive power control capability. The other voltage control devices available are OLTC and VR. The VR operates in an autonomous mode. It consists of normally open switch which connects to an alternate power feeding point. A grid integrated PV model. The converter control achieves the best possible active power capture through MPPT. Fig.7 shows the equivalent circuit of the MV distribution feeder. There is a possibility of power flows in the reverse direction towards the source substation OLTC, particularly when PV penetration is high.

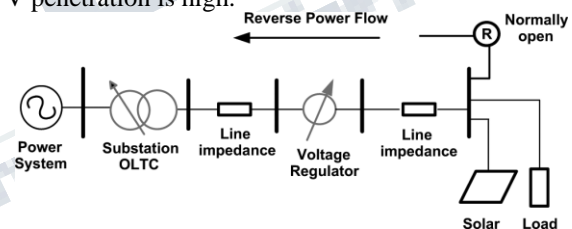


Fig. 7. Radial system topology.

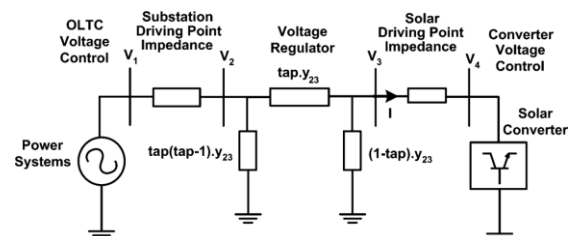


Fig. 8. Equivalent circuit of a radial system with VR.

III. SIMULATION RESULTS

The UKGDS system considers two DGs at bus 18 and 89. The PV generation plants are considered at the same locations. The VR is considered in an autonomous mode. Both OLTC and PV generation plants are coordinated to achieve the voltage control.

The objective function guarantees reduced tap counts and reduced operation of VR in non preferred zone in a preferential manner formulated using weighted combinations. The scalar weights W_c and W_r are varied such that $W_c + W_r = 1$. Table 2 demonstrates simulation results for different values of weights. In Table 2, VR1 represents VR connected between bus 54 and 75, and VR 2 represents VR connected between bus 24 and 23. Parameters for the penalty function are chosen such that, the penalty function value should not be too small or too large as compared to base case tap count objective function when equal weights are assigned for both objective functions. At the end of the control range for the voltage regulator (at tap position ± 16), the penalty value is significantly higher than the tap count objective function (when the weight W_r corresponding to the voltage regulator runaway is non zero). This ensures that even for the smaller value of W_r the voltage regulator operation at absolute limit is avoided. In order to maintain the control margin for the voltage regulator and avoid runaway, a higher tap non-preferred zone is defined. The preferred zone for both VR is considered to be between tap positions +10 to -10. Case 1 is considered at unity power factor non-coordinated operation. It can be observed that in Case 1 the total number of tap count is 76 and number of operations of VR1 in the non preferred zone is 11 and that for VR2 is 8. The next case demonstrates the minimization of tap operation in the non preferred zone.

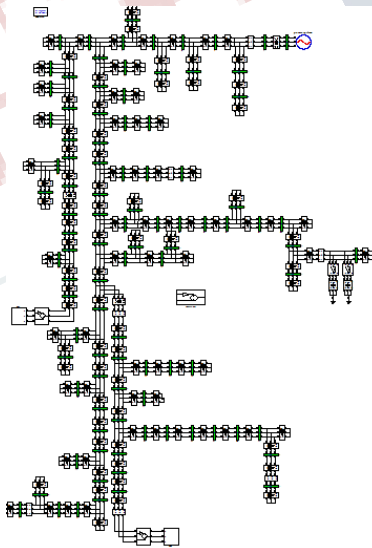


Fig.9. UKGDS IEEE-95 bus system simulation model with two switched capacitor bank at bus 52

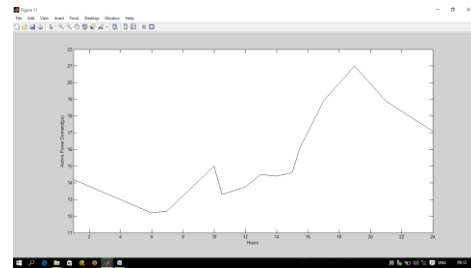


Fig.10: UKGDS system load profile

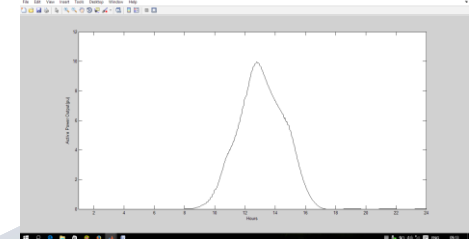


Fig.11: Solar active power profile

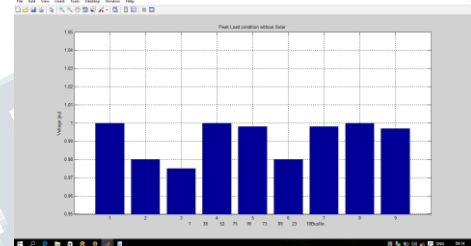


Fig.12. UKGDS system voltages during peak load condition without PV (nominal voltage at bus 1)

The weight W_r is set to 1 and no weight is attached to tap counts. It can be observed that all the operation of the VR1 occurs in preferred zone. But the total tap count remains 61 which is high. In the third case weight W_c is set to 1 and no weight is attached to the penalty function. Tap counts are reduced to 33 but tap operation instances in the non preferred zone are 9 for VR1 and 12 for VR2. This case demonstrates the benefits of penalty function. Conventional objective functions do not consider the proposed penalty. It can be observed that though tap counts are reduced, tap operation happens close to its limit. Case 4 gives the most satisfactory value of the objective function. The following step by step procedure is considered while tuning weights.

Step 1: There are two objectives: tap counts minimization and avoiding operation in the non preferred zone. Tap count minimization is considered to be the preferred objective in this study. The weight tuning is done in preferential manner, so intuitively

weight assigned for tap count minimization W_c has to be higher.

Step 2: W_c is set to 1 and W_r to 0 and the best possible objective value of the tap count is calculated. Table 2 shows the values achieved.

Step 3: W_r is set to 1 and W_c to 0 and the best possible objective value of the tap in the preferred zone is calculated. Table 2 shows the values achieved.

Step 4: The target reduction in tap counts from the base case is decided. In this simulation study it is considered 50.

Step 5: The values of W_c are varied in steps of 0.1 from 0 to 1. The values of both objective functions are noted. Fig.18 shows the variation in both objective function values. Case 1 tap count is 76, considering target tap count reduction to 50, the weight range selected is W_c from 0.6 to 1.

Step 6: While selecting the final value of W_c (from 0.6 to 1) along with the frequency of operation of voltage regulators in non preferred zone, the voltage regulator control margin is also considered. The control margin of a voltage regulator is defined as the difference between the voltage regulator limit and the nearest operation of the voltage regulator to its limit.

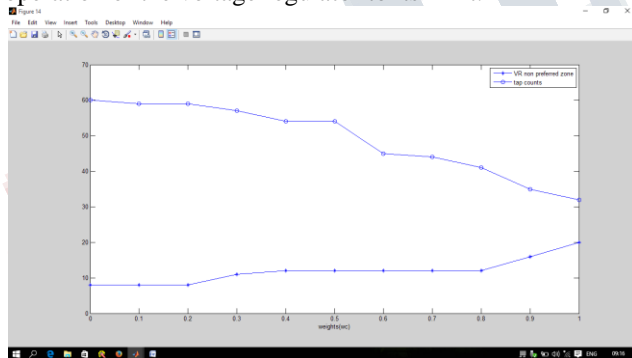


Fig.13. Variation in both objective function values at different weights.

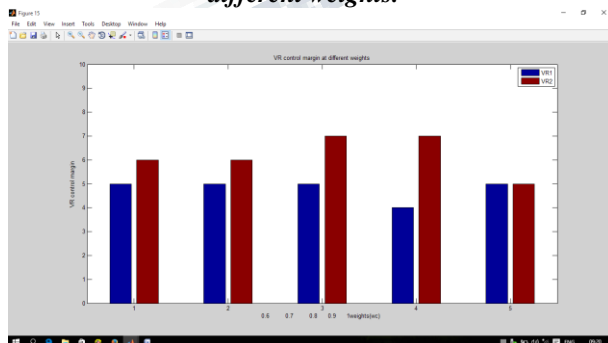


Fig.14. VR control margin at different weights

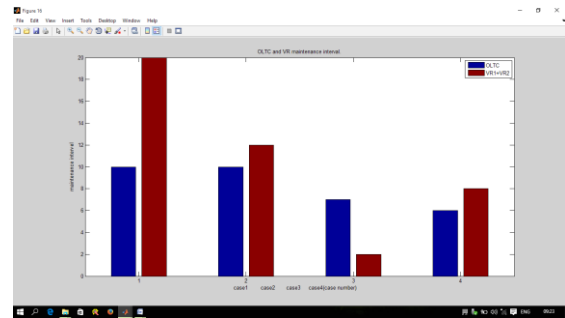


Fig.15. OLTC and VR maintenance interval

Step 7: The voltage regulator preferred zone of operation is considered between tap values +10 to -10. Hence a value above 6 is a good control margin. For every value of weight W_c from 0.6 to 1, the control margin for both voltage regulators is plotted. Above figures demonstrate the control margin for both VR in the system.

Step 8: It can be observed from Figures that W_c equal to 0.8 offers the same number of tap operations in non preferred zone as W_c equal to 0.7 and the same control margin as can be achieved by W_c equal to 0.9, hence the final selection of weights is W_c is equal to 0.8 and W_r is equal to 0.2. Thus the final optimal weight tuning is achieved for Case 4 of Table 2.

Table 2: UKGDS 95 bus system performance

Case	Weights		Tap Count				Operation in non preferred zone		
	W_c	W_r	OLTC	VR1	VR2	Total	VR1	VR2	Total
1	-	-	40	19	17	76	11	8	19
2	0.0	1.0	40	4	17	61	0	8	8
3	1.0	0.0	29	2	2	33	9	12	21
4	0.8	0.2	25	14	2	41	12	0	12

Table 3: Percentage reduction in OLTC and VR tap count

Case	2	3	4
OLTC	0%	27.5%	37.7%
VR1+VR2	41.66%	88.9%	55.56%

Table 4: OLTC and VR Set Points

	Set points	Dead band
OLTC	1.01	0.02
VR1,VR2	1.02	0.02

Table 5: Tap count with no reactive power support from solar at zero irradiance

OLTC	VR1	VR2	TOTAL
29	10	11	50

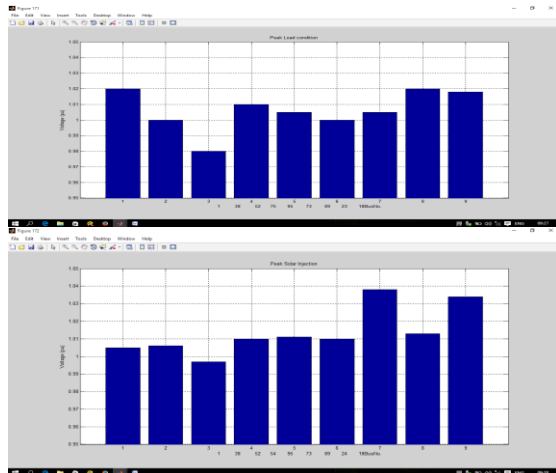


Fig16. Voltages during peak load condition and peak solar injection at different buses (Optimal case $W_c = 0.8$ and $W_r = 0.2$)

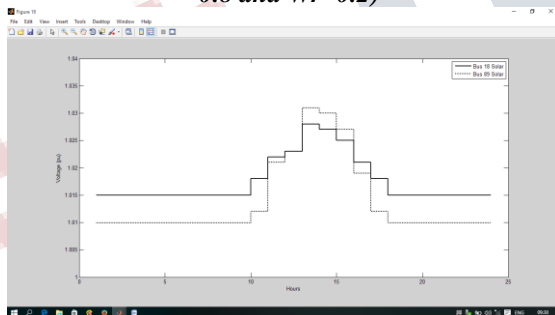


Fig17. Hourly PV plant voltage setpoints

The results of Table 2 are confirmed with 30 sec time step load flow. Table 3 shows the percentage reduction in the OLTC and VR tap counts. Typical life of transformer and VR is 30 years. The typical maintenance interval of OLTC and VR is after 3 years. So in the base case, a total of 10 maintenance schedules are considered for each VR and OLTC. Figure shows a reduction in maintenance intervals for this test system if the daily percentage reduction as in Table 3 is achieved. Figures shows voltage values at different buses for Case 4 during the peak solar injection and the peak load. It can be observed that in both operating conditions, the voltage profile across the feeder is maintained within $\pm 5\%$. Table 4 shows OLTC and VR set points. The

hourly voltage set points for both PV plants are shown in Figures. Table 5 demonstrates Case 3 for which W_c is 1 and W_r is 0. The comparison with case 3 in Table 2 shows that, there is significant increase in tap counts when no reactive power support is considered from PV at zero irradiance. The operation of both PV plants for a particular day under consideration is represented in Figure. The active power and apparent power consumption of both the PV plants is represented in Figure. The solid line represents the inverter capacity. Figure demonstrates sufficient reactive power margin available at all the operating values. Also PV plant operates at MPPT at all instants. As can be observed from Figure, there are in total 24 optimal voltage set points calculated. It can be observed from Figure that the voltage at bus 52 is acceptable but lower during peak load condition. Distribution feeders are equipped with switched capacitor at bus 52.

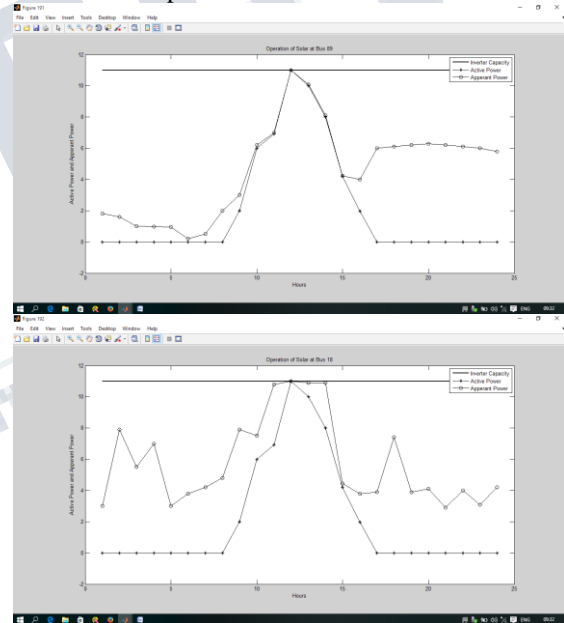


Fig. 18. PV plant operation

The simulation model of the UKGDS IEEE 95-bus system with two switched bank capacitors is shown in Figure. The capacitor bank C1 and C2 each has rating of 200 kVAr at rated voltage (1pu). This will ensure that voltage at bus 52 is 1pu. Both VR and capacitor are in autonomous mode. So, based on the daily load and irradiance profile, OLTC and PV reactive power set points are coordinated. Again similar to the base case, scalar weights W_c and W_r are varied such that $W_c + W_r = 1$. Table 6 demonstrates

simulation results for base case and optimal case. Figure shows the PV plant voltage set points for the optimal it can also be seen from figures that voltages at all buses remain within the prescribed limits.

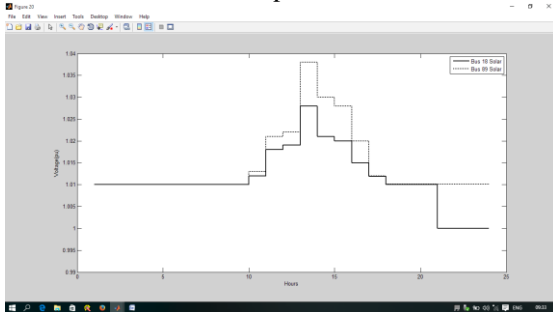


Fig.19: PV plant voltage setpoints with capacitors at bus 52

The following advantages are observed with the inclusion of capacitor:

- The number of tap counts to achieve voltage control is lower when capacitors are placed at Bus 52.
- The number of operations of the voltage regulator in the non preferred zone is reduced with the presence of capacitor.

IV. CONCLUSION

The active power injection at unity power factor by PV impacts the operation of OLTCs and VRs mechanisms and non-coordinated reactive power control in distribution system. This paper has proposed strategy ensures minimum number of tap counts of the OLTCs and VRs and mitigates the runaway. The strategy defines the non preferred zone of operation around the VR extreme tap values to avoid runaway. The strategy coordinates various voltage control devices and the PV generation reactive power support mode. The proposed reactive power coordination strategy is effective in minimizing tap counts, avoiding the runaway and maintaining the feeder voltage within the specified limits. Further system also considers a night time reactive power support from PV inverters. It is found that tap operations can be minimized by utilizing reactive power support capabilities of PV inverters when PV active power output is zero. This paper concluded that voltage regulation strategies in the presence of PV generation will be useful to distribution network operators. The strategies can be utilized in designing various voltage control devices set points and

deciding control settings of OLTCs, VRs and PV generators etc during daily operation of a distribution feeder.

REFERENCES

- [1] "Global market outlook for photovoltaics until 2016," May 2012 [On-line]. Available: <http://www.epia.org/>
- [2] Shaaban, M.F.; Atwa, Y.M. ; El-Saadany, E.F. "DG allocation for benefit maximization in distribution networks," IEEE Transactions on Power Systems, Vol. 28, no.2 ,pp. 639 – 649, May. 2013.
- [3] R. Tonkoski, L. Lopes, and T. EL-Fouly, "Coordinated active power curtailment of grid connected pv inverters for overvoltage prevention," IEEE Trans. Sustain. Energy, vol. 2, no. 2, pp. 139–147, Apr. 2011.
- [4] A. G. Madureira and J. A. P. Lopes, "Voltage and reactive power control in MV networks integrating microgrids," Proc. ICREPQ, vol. 7, pp. 1–5, 2007.
- [5] L. M. Cipcigan and P. C. Taylor, "Investigation of the reverse power flow requirements of high penetrations of small-scale embedded generation," IET Renewable Power Gen., vol. 1, no. 3, pp. 160–166, 2007.
- [6] F. A. Viawan and D. Karlsson, "Voltage and reactive power control in system with synchronous machine-based distributed generation," IEEE Trans. Power Del., vol. 23, no. 2, pp. 1079–1087, Apr. 2008.
- [7] R. A. Walling and K. Clark, "Grid support functions implemented in utility-scale PV system," in Proc. IEEE PES Transm. Distrib. Conf. Expo., 2010, pp. 1–5.
- [8] S. Civanlar and J. J. Grainger, "Forecasting distribution feeder loads: Modeling and application to Volt/Var control," IEEE Trans. Power,Del., vol. 3, no. 1, pp. 255–264, Jan. 1988.
- [9] M. Liu, S. K. Tso, and Y. Cheng, "An extended nonlinear primal dual interior-point algorithm for reactive-power optimization of large scale power system with discrete control variables," IEEE Trans. Power Syst., vol. 17, no. 4, pp. 982–991, Nov. 2002.
- [10] A. Malekpour and A. Pahwa, "Reactive power and voltage control in distribution system with photovoltaic generation," in Proc. IEEE North Amer. Power Symp., 2012, pp. 1–6.